Korean J. Chem. Eng., **27**(4), 1333-1337 (2010)
DOI: 10.1007/s11814-010-0179-6

Comparison of amine-functionalized mesoporous silica particles for ibuprofen delivery

Kitae Lee*, Deokkyu Lee*, Hosub Lee*, Chang-Koo Kim, Zhijian Wu***,****, and Kangtaek Lee*,†**

*Department of Chemical and Biomolecular Engineering, Yonsei University, Seoul 120-749, Korea
**Department of Chemical Engineering and Division of Energy Systems Research, Ajou University, Suwon 442-749, Korea
***Key Laboratory of Salt Lake Resources and Chemistry, Qinghai Institute of Salt Lakes,
Chinese Academy of Sciences, Xining 810008, China
****The Key Laboratory for Functional Materials of Fujian Higher Education,
College of Materials Science and Engineering, Huaqiao University, Quanzhou 362021, China
(*Received 24 September 2009 • accepted 11 November 2009*)

Abstract−We have prepared three different types of amine-functionalized silica particles: i) mesoporous silica (MESO1); ii) nonporous core-mesoporous shell silica (MESO2); iii) SBA-15 particles. Scanning electron microscopy (SEM), transmission electron microscopy (TEM), and nitrogen sorption experiment were used to study the morphology of the synthesized particles. To investigate the drug loading and subsequent release of the particles, ibuprofen was used as a model drug for oral delivery. Loading capacity of the particles in this work was found to be higher than that in the previous studies, and followed the order of MESO1>MESO2>SBA-15 particles. Release experiments showed the similar release rate for MESO1 and MESO2 particles from which only <40% of ibuprofen was released after 5 h. From SBA-15 particles, however, more than 80% of ibuprofen was released in 5 h at pH 4 and 7.4. Ibuprofen release from SBA-15 was slowest at pH 2 (~pH of stomach body) and fastest at pH 7.4 (~pH of proximal intestine). Difference in release rates was ascribed to the different morphology and pore structure of the carrier particles.

Key words: Mesoporous, Silica, Ibuprofen, Loading, Release

INTRODUCTION

Over the past three decades there has been a rapid growth in sustained/controlled drug delivery in the fields of modern medicine and pharmaceuticals because it can bring both therapeutic and commercial values to health-care products [1]. In controlled release, drug carriers play a critical role for loading and release of the drug.

Recently, silica-based materials have widely been studied as drug release carriers [2]; these include i) silica-based xerogels; ii) mesoporous silica-based materials such as MCM-41 (Mobile Crystalline Materials) and SBA-15 (Santa Barbara Amorphous type material); iii) mesoporous hollow silica spheres [3]. Among these silica-based materials, mesoporous silica-based materials such as MCM-41 and SBA-15 have been proposed as carriers for both drug and gene delivery [4,5] because they can be synthesized as a highly ordered mesoporous materials that contain unidimensional pores with a uniform size ranging from about 2 to 8 nm and their synthesis is relatively easy compared to other mesoporous hollow silica spheres.

When mesoporous silica-based materials are used as carriers for drug release, several factors such as pore size distribution, morphology, and surface functionality of the carriers can affect the release behaviors. For instance, pore size has a pronounced effect on the kinetics of drug release: drug delivery rate decreases with the decrease of the pore size [6]. Even if the difference in pore size between two mesoporous silica materials was as small as 0.2 nm, the discrepancy in the release rate was quite evident [7]. Morphology has a significant effect on the interface between drug-carrying particles and fluids, and could thereby affect kinetics of drug release [4]. It was shown that one-dimensional or three-dimensional "cage-like" pore structure with small pore openings of mesoporous silica could greatly reduce the drug release rate [6]. Functionalization of the carriers would also potentially affect release rate by affecting the drug binding strength [4]: increased affinity of the host-guest by the organically functionalized mesoporous silica could lead to slower release of drug [6,8].

Although there have been reports on the effects of pore size, morphology, and functionalization of mesoporous silica-based materials on drug release, few reports are available that compare the drug loading and release characteristics of the mesoporous silica carriers with the same surface group, but different morphology. Here, we prepare three different types of amine-functionalized mesoporous silica particles to compare the loading and release characteristics of ibuprofen.

Ibuprofen belongs to a group of nonsteroidal anti-inflammatory drugs. It works by reducing hormones that cause inflammation and pain in the body and is used to reduce fever and treat pain or inflammation caused by many conditions such as headache, toothache, back pain, or minor injury [6]. Ibuprofen is frequently employed as a model drug for controlled delivery owing to its suitable molecule size of about $1.0\times0.5\ nm^2$, good pharmacological activity, and short biological half-life (2 h) [1]. Molecular structure of ibuprofen is shown in Fig. 1.

In this work, we first synthesized three different types of mesoporous silica particles, *i.e.*, mesoporous silica (MESO1), nonporous core-mesoporous shell silica (MESO2), and SBA-15 particles, and functionalized their surface with amine groups. Scanning electron microscopy (SEM), transmission electron microscopy (TEM), nitrogen sorption, and zeta potential measurements were used to char-

†To whom correspondence should be addressed.
E-mail: ktlee@yonsei.ac.kr

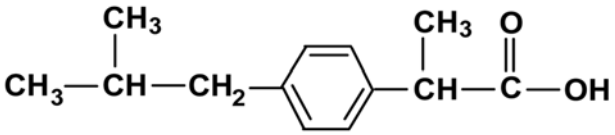

Fig. 1. Molecular structure of ibuprofen.

acterize the synthesized particles. We then used these particles as carrier materials for oral delivery of ibuprofen and compared their loading and release characteristics in different conditions.

EXPERIMENTAL

1. Materials

Tetraethoxysilane (TEOS), Pluronic 123 triblock copolymer [poly(ethylene glycol)$_{20}$-poly(propylene glycol)$_{70}$-poly(ethylene glycol)$_{20}$] (MW: ~5800), and APTES (3-aminopropyl triethoxysilane) were purchased from Aldrich. Ibuprofen (minimum 98% GC) and CTAB (hexadecyltrimethylammonium bromide 99%) were purchased from Sigma and ACROS, respectively. Hydrochloric acid, sodium hydroxide, ethyl alcohol, and ammonium hydroxide were purchased from Duksan Co., and hexane and PBS (phosphate buffered saline) buffer were purchased from Showa Co. and Invitrogen Co., respectively. All chemicals were used without further purification.

2. Synthesis of the Mesoporous Silica Particles

2-1. Amine-functionalized Mesoporous Silica (MESO1) Particles

Amine-functionalized mesoporous silica particles (MESO1) were synthesized according to the recipe by Lai et al. [5]. First, we dissolved 1 g of CTAB in 480 g of distilled and deionized water, and added 3.5 mL of 2 M NaOH solution. This solution was heated for 30 min at 80 °C. We then quickly added 5 mL of TEOS and 0.99 mL of APTES to the solution and reacted for 2 h at 80 °C with stirring, which produced white solid precipitates. As a control, unmodified mesoporous silica particles were also synthesized without APTES addition. The suspension was cooled to room temperature, and the precipitates were separated by filtration, washed with distilled water and methanol, and vacuum dried at 80 °C for 12 h. Surfactants were removed by heating the precipitates in ethanol for 24 h at ~80 °C under reflux.

2-2. Amine-functionalized Nonporous Core-Mesoporous Shell Silica (MESO2) Particles

To produce nonporous core, 1.1 mL of ammonium hydroxide solution (NH_4OH, 28 wt%) was added to a solution containing 35 mL of ethanol and 13 mL of distilled water. After stirring for 30 min, we added 5.6 mL of TEOS to the solution and stirred for 6 h at room temperature, which produced the nonporous core silica spheres with uniform size. 40 mL of the suspension was centrifuged to separate particles, and these particles were redispersed in a solution containing 3 mL of H_2O, 36.25 mL of EtOH, and 0.75 mL of NH_4OH.

Mesoporous shell was then formed on the silica spheres by adding additional H_2O, CTAB, and TEOS as reported by Yoon et al. [9]. We diluted 20 mL of the suspension with 40 mL of H_2O, and quickly added 6 mL of CTAB surfactant solution (110 mM, dissolved in an H_2O/EtOH mixture at 2 : 1 volumetric ratio) under vigorous stirring. After stirring for 30 min, 0.6 mL of TEOS was added to the reaction mixture. The solution was reacted at room temperature for 18 h and centrifuged, and the particles were dried at 70 °C for 18 h. The surfactants were removed by heating the particles in ethanol at ~80 °C for 24 h under reflux. The resulting particles were then separated by centrifugation, washed with excess water, and dried at 70 °C for 12 h.

To functionalize the particle surface with the amine groups, we added 1 g of particles to the solution containing 1 mL of APTES and 50 mL of ethanol, and reacted at ~80 °C for 12 h under reflux. After the reaction, the particles were separated by centrifugation, washed with a large amount of water, and dried at 70 °C for 12 h.

2-3. Amine-functionalized SBA-15 Particles

SBA-15 was prepared using the procedures reported by Zhao et al. [10] and Brodie-Linder et al. [11]. 1.4 g of Pluronic 123 triblock copolymer was dissolved in a solution containing 50 mL of water and 5.52 mL of HCl (38 wt%). After stirring for 3 h at room temperature, we added 3.44 g of TEOS. The solution was vigorously stirred for 10 min and reacted at 40 °C for 24 h under static condition, followed by aging at 100 °C for 24 h. To remove the copolymer, precipitates were soaked in ethanol for 12 h. The particles were then separated by centrifugation, washed with distilled water, and dried at 70 °C for 12 h.

For functionalization with the APTES, the same procedure used for the MESO2 particles was used.

3. Characterization

Textural properties of the mesoporous silica were determined by using the nitrogen sorption experiment. The adsorption/desorption isotherm of nitrogen at 77 K was measured with a Micromeritics ASAP 2020 analyzer. Prior to the measurements, the mesoporous silica particles were degassed for 6 h at 120 °C. The specific surface area was calculated from the BET equation and the pore size and volume were calculated by BJH method based on the desorption branch of the isotherm. To observe the size and morphology of particles, scanning electron microscopy (SEM) and transmission electron microscopy (TEM) experiments were performed using the JEOL JSM6500-Fmicroscope and JEOL JEM-2100 microscope, respectively. Zeta potential of the synthesized particles was measured with a Malvern Zetasizer Nano ZS.

4. Ibuprofen Loading and Release Experiments

To load ibuprofen on mesoporous silica particles, 0.17 g of dried particles were added to 10 mL of hexane-ibuprofen solution (25 mg/mL) and soaked for 3 days under stirring. Ibuprofen concentration in solution was monitored by using a Shimadzu UV-1650 spectrophotometer at a wavelength of 272 nm. Amount of the drug loaded onto particle was measured by the change in the UV intensity before and after loading. The particles were separated by centrifugation and dried at 100 °C in the oven.

For the release experiments, we added 0.017 g of ibuprofen-loaded particles in 10 mL of phosphate buffer solution at pH values of 2, 4, and 7.4 under minimum stirring. Temperature during release experiments was kept at 37 °C to simulate the human body. Amount of the released ibuprofen was estimated by using a UV spectrophotometer at a wavelength of 273 nm.

RESULTS AND DISCUSSION

1. Characterization of the Synthesized Mesoporous Silica Particles

Fig. 2 compares the scanning electron microscopy (SEM) images

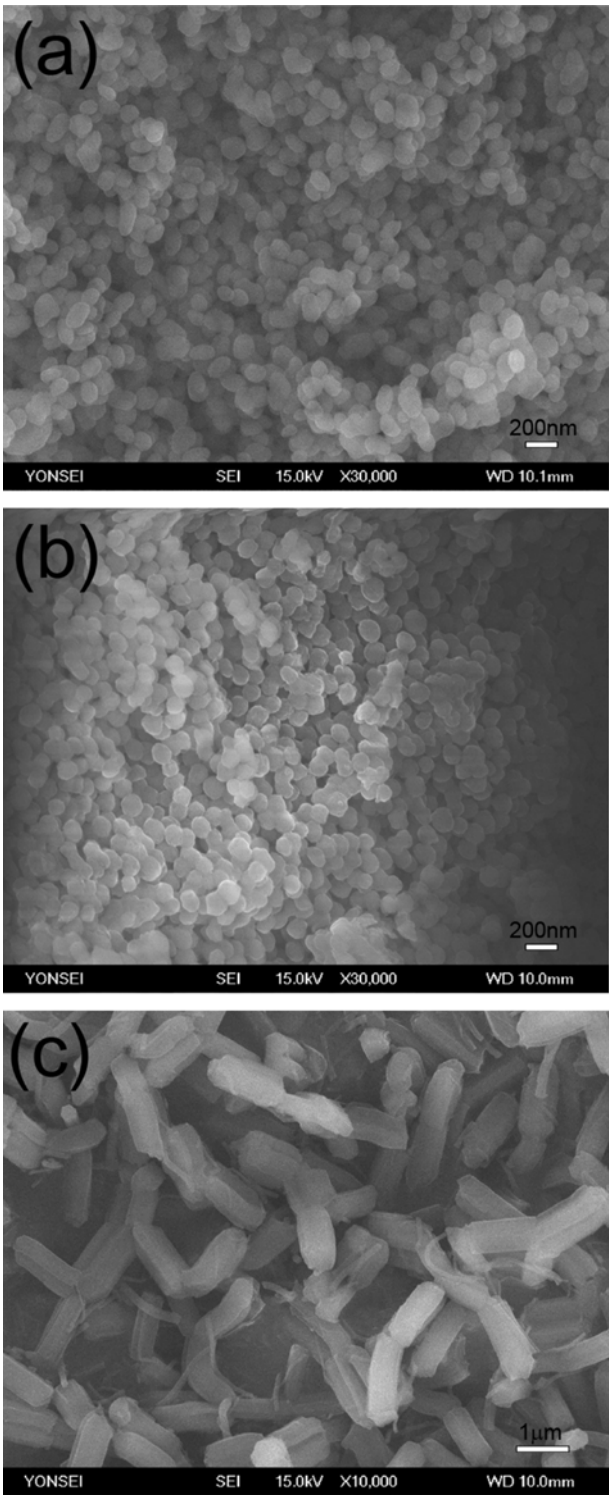

Fig. 2. SEM images of the unfunctionalized mesoporous silica particles: (a) MESO1; (b) MESO2; (c) SBA-15.

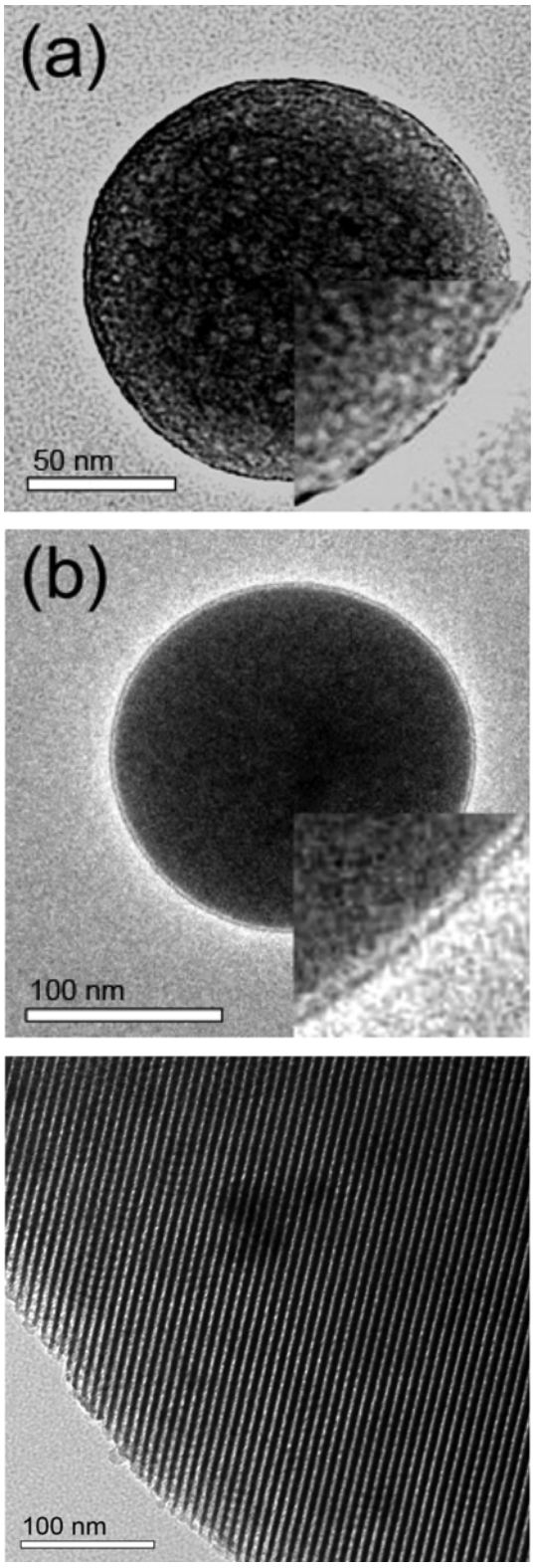

Fig. 3. TEM images of the unfunctionalized mesoporous silica particles: (a) MESO1; (b) MESO2; (c) SBA-15.

of the synthesized particles. MESO1 (Fig. 2(a)) and MESO2 particles (Fig. 2(b)) have a spherical shape with a diameter of *ca.* 130 nm. Fig. 2(c) shows that SBA-15 particles have a rod-like shape with a relatively uniform length of *ca.* 1.5 μm. TEM was also used to study the microstructure of the particles as shown in Fig. 3. Figs. 3(a) and 3(b) clearly show the mesoporous structure inside the MESO1 and in the shell of the MESO2 particles, respectively. Cylindrical mesopores are also evident in the SBA-15 particles as shown in Fig. 3(c).

The surface of these particles has been functionalized with APTES because ionic interaction between amine groups on the silica sur-

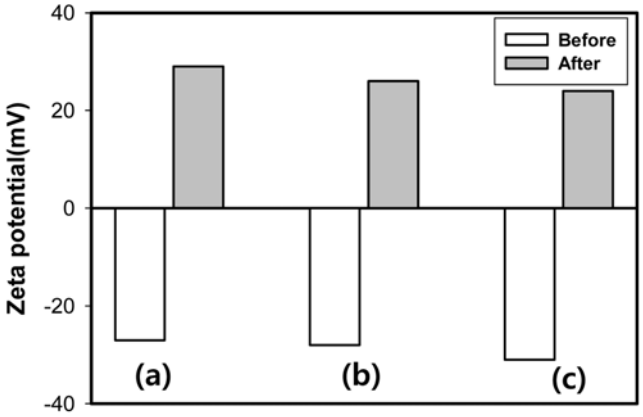

Fig. 4. Change in zeta potential after surface modification with APTES: (a) MESO1; (b) MESO2; (c) SBA-15.

Table 1. Textural properties of three types of mesoporous silica particles before and after surface modification with APTES

Materials		Surface area (m^2/g)	Pore volume (cm^3/g)	Pore size (nm)
MESO1	Unfunctionalized	712.8	0.47	2.3
	Functionalized	499.6	0.39	2.8
MESO2	Unfunctionalized	296.6	0.31	5.2
	Functionalized	248.7	0.28	9.2
SBA-15	Unfunctionalized	610.1	0.83	5.4
	Functionalized	282.6	0.49	6.9

Table 2. Ibuprofen loading capacity of the synthesized particles

Materials	MESO1	MESO2	SBA-15
Loading (%)	98.8	84.0	77.0

face and carboxylic groups of ibuprofen (Fig. 1) can help loading of ibuprofen. To confirm the presence of amine groups on the particle surface after functionalization, zeta potential of particles was measured before and after surface modification. Fig. 4 demonstrates that in all cases the zeta potential increased substantially from negative to positive value after surface functionalization due to amine groups on surface, confirming a successful functionalization.

Textural properties of these particles are also summarized in Table 1. Surface modification caused a decrease in both pore volume and BET surface area and increase in pore size probably because the amine groups on the surface interfered with the nitrogen adsorption [12]. Note that SBA-15 particles exhibited the most significant change in textural property after surface modification with amine groups.

2. Ibuprofen Loading and Release

To use the mesoporous silica particles as carriers for drug release, we loaded ibuprofen onto the particles. According to the dimension of ibuprofen ($1.0\times0.5\ nm^2$) [6], pores of all particles are large enough to accommodate ibuprofen. It was shown that the extent of drug-loading is related to BET surface area, pore size, and surface property of mesoporous silica [6]. Table 2 compares the ibuprofen loading capacity of these particles. Loading capacity is defined as the amount of the loaded ibuprofen with respect to the amount of ibuprofen used in the loading experiment. Note that the loading capacity of the particles synthesized in this work was higher than the previously reported values [13-15]. MESO1 particles showed the highest loading capacity, which can be attributed to the largest surface area after surface modification. Loading capacity of MESO1 particles was higher than that of MESO2 particles because MESO2 particles had nonporous core, which is also responsible for larger

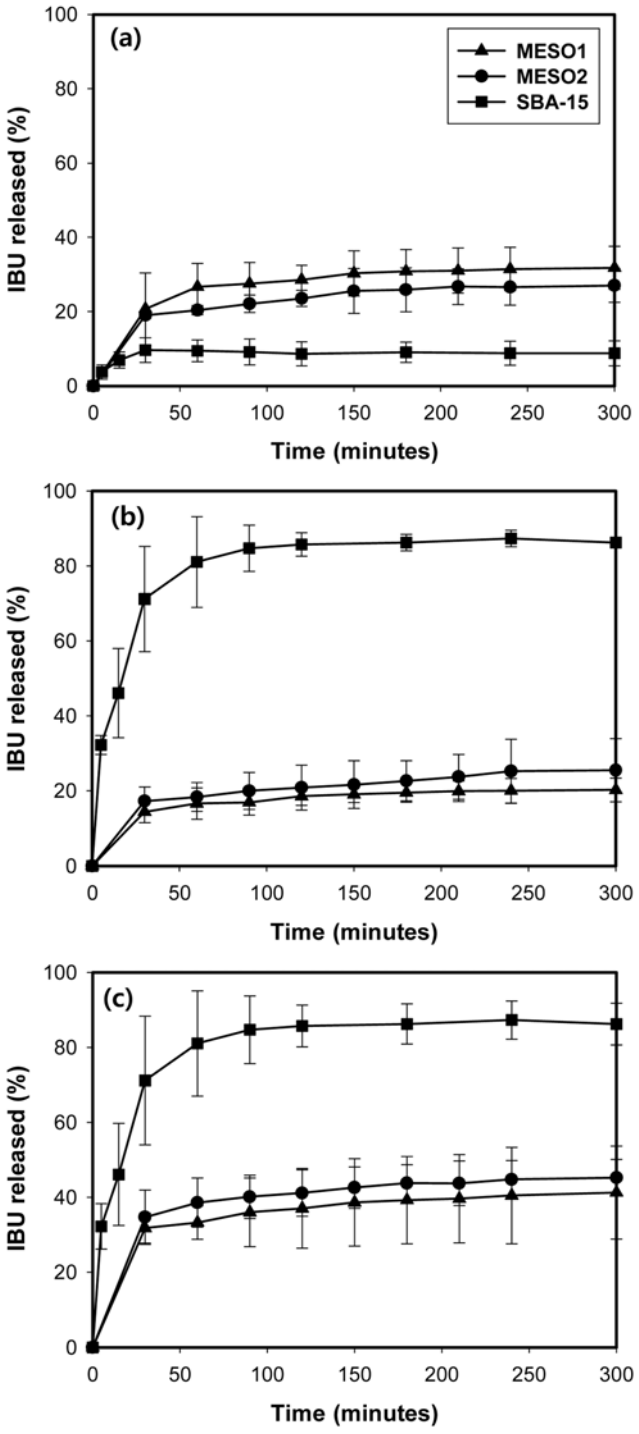

Fig. 5. Ibuprofen release profiles (%) at different pH values: pH= (a) 2; (b) 4; (c) 7.4.

surface area and pore volume of MESO1 particles. Although SBA-15 particles had higher surface area and pore volume than MESO2 particles, the amount of ibuprofen loading was smaller than that of MESO2 particles. Since all types of particles have the same functional group and basic matrix composition (*i.e.*, mainly silica), interaction between particles and drug should also be similar. We thus suspect that difference in the particle morphology is responsible for the difference in loading capacity.

In oral delivery, ibuprofen is known to be absorbed mainly in the stomach and proximal intestine and its pKa value is ~4.4 [1]. The pH in the human body changes from 1-2 in the stomach body to 5-7 in the antrum, and 7-8 in the proximal intestine [16,17]. Thus, we performed the release experiments at pH values of 2, 4, and 7.4.

Fig. 5 compares the release profiles of ibuprofen at different pH values. Note that the released amount is expressed in the wt% of the ibuprofen released from the initially loaded amount. At pH 2, which is close to the pH of stomach body, ibuprofen release was very slow (*i.e.*, less than 40% released even after 5 h) in all cases; MESO1 and MESO2 particles showed the similar release rates while the release from SBA-15 particle was slowest. The release rate was even slower for the MESO1 and MESO2 particles at pH 4 while it was much faster for SBA-15 particles (*i.e.*, >80% released in 5 h). At pH 7.4, which is close to the pH of proximal intestine, ibuprofen release was fastest for all particles, even though the released amount of MESO1 and MESO2 particles after 5 h was only half (~40%) of the SBA-15 particles.

Based on the molecular structure and pKa value of ibuprofen, it exists mainly as an anion at high pH (7.4), but in unionized form at low pH (2 and 4). Therefore, solubility should increase with pH, which may be responsible for faster release of ibuprofen at high pH (7.4).

Furthermore, the release rate from MESO1 and MESO2 particles was almost indistinguishable under the same condition. Because interaction between particles and drug should be similar for all particles, it is reasonable to expect that the difference in the release rate comes mainly from different morphology and pore structure of the particles. Based on Figs. 2 and 3, SBA-15 particles show much different morphology from those of MESO1 and MESO2 particles. We suspect that the cylindrical pores of SBA-15 particles provide easier access for ibuprofen molecules than the tortuous pores in MESO1 and MESO2 particles, and thus are responsible for much faster release at pH 4 and 7.4.

CONCLUSIONS

We have prepared three different types of the amine-functionalized mesoporous silica particles and compared them as carriers for the controlled release of ibuprofen. The results can be summarized as follows:

(i) MESO1 and MESO2 particles have a spherical shape with *ca.* 130 nm in diameter while SBA-15 particles have a rod-like shape with a relatively uniform length of *ca.* 1.5 μm.

(ii) Surface modification of all particles decreases both the pore volume and BET surface area, but increases the pore size. MESO2 particles show the smallest surface area and pore volume because of their nonporous cores.

(iii) The loading capacity of the particles synthesized in this work is higher than the previously reported values. The loading capacity of the functionalized particles follows the order of MESO1>MESO2> SBA-15 particles.

(vi) MESO1 and MESO2 particles exhibit similar ibuprofen release rate at all pH values. At pH 4 and 7.4, SBA-15 particles show much faster release than MESO1 and MESO2 particles. Ibuprofen release from SBA-15 particles is slowest at pH 2 (~pH of stomach body) and fastest at pH 7.4 (~pH of proximal intestine).

We suspect that the difference in the release rate is probably caused by the different morphology and pore structure of the particles. Thus, by mixing particles with different morphology that exhibit different loading and release behaviors, we may be able to control the drug release rate in different conditions.

ACKNOWLEDGEMENTS

This work was financially supported by NRF through the Nano R&D program (2009-0082417) and the Grant No. R01-2007-000-20821-0. Z. Wu acknowledges the Natural Science Foundation of Fujian Province of China (No. E0710016), and the foundation of Knowledge Innovation Program of Chinese Academy of Sciences (kzcx2-yw-115).

REFERENCES

1. F. Qu, G. Zhu, H. Lin, J. Sun, D. Zhang, S. Li and S. Qiu, *Eur. J. Inorg. Chem*., **2006**, 3943 (2006).
2. M. Vallet-Regí, F. Balas and D. Arcos, *Angew. Chem. Int. Ed.*, **46**, 7548 (2007).
3. Z. Wu, Y. Jiang, T. Kim and K. Lee, *J. Control. Release*, **119**, 215 (2007).
4. M. Manzano, V. Aina, C. O. Areán, F. Balas, V. Cauda, M. Colilla, M. R. Delgado and M. Vallet-Regí, *Chem. Eng. J*., **137**, 30 (2008).
5. C.-Y. Lai, B. G. Trewyn, D. M. Jeftinija, K. Jeftinija, S. Xu, S. Jeftinija and V. S.-Y. Lin, *J. Am. Chem. Soc*., **125**, 4451 (2003).
6. F. Qu, G. Zhu, H. Lin, W. Zhang, J. Sun, S. Lia and S. Qiu, *J. Solid State Chem*., **179**, 2027 (2006).
7. W. Xu, Q. Gao, Y. Xu, D. Wu, Y. Sun, W. Shen and F. Deng, *Powder Technol*., **191**, 13 (2009).
8. W. Xu, Q. Gao, Y. Xua, D. Wu, Y. Sun, W. Shen and F. Deng, *J. Solid State Chem*., **181**, 2837 (2008).
9. S. B. Yoon, J. B. Kim, J. H. Kim, Y. J. Park, K. R. Yoon, S. K. Park and J. S. Yu, *J. Mater. Chem*., **17**, 1758 (2007).
10. D. Zhao, J. Feng, Q. Huo, N. Melosh, G. Fredrickson, B. Chmelka and G. Stucky, *Science*, **279**, 548 (1998).
11. N. Brodie-Linder, G. Dosseh, C. Alba-Simonesco, F. Audonnet, M. Impéror-Clerc, *Mater. Chem. Phys*., **108**, 73 (2008).
12. J. C. Doadrio, E. M. B. Sousa, I. Izquierdo-Barba, A. L. Doadrio, J. Perez-Pariente and M. Vallet-Regí, *J. Mater. Chem.*, **16**, 462 (2006).
13. S. Huh, J. W. Wiench, J.-C. Yoo, M. Pruski, V. S.-Y. Lin, *Chem. Mater*., **15**, 4247 (2003).
14. C. Barbé, J. Bartlett, L. Kong, K. Finnie, H. Lin, M. Larkin, S. Calleja, A. Bush and G. Calleja, *Adv. Mater*., **16**, 1959 (2004).
15. M. Vallet-Regi, A. Rámila, R. P. del Real and J. Pérez-Pariente, *Chem. Mater*., **13**, 308 (2001).
16. G. Yakovlev, *Biomed. Eng*., **38**, 292 (2004).
17. B. Lönnerdal, *J. Am. Coll. Nutr*., **21**, 218S (2002).